Observation of a High-Density Ion Mode in Tokamak Microturbulence

D. L. Brower, W. A. Peebles, S. K. Kim, and N. C. Luhmann, Jr.
Institute of Plasma and Fusion Research, University of California, Los Angeles, California 90024

W. M. Tang
Plasma Physics Laboratory, Princeton University, Princeton, New Jersey 08544

and

P. E. Phillips
Fusion Research Center, University of Texas at Austin, Austin, Texas 78712
(Received 24 April 1987)

For high-density Ohmic discharges in the Texas Experimental Tokamak (TEXT), a distinct ion mode (i.e., density fluctuations propagating in the ion diamagnetic drift direction) is observed in the microturbulence spectra. The magnitude and spectral characteristics of this mode are identified. Onset of the ion feature occurs at plasma densities where a clear saturation is evident in the global energy-confinement time τ_E. A possible connection between this experimentally observed ion mode and the theoretically predicted properties of instabilities driven by ion temperature gradient (η_i) is explored.

PACS numbers: 52.35.Kt, 52.35.Mw

Previous measurements on the Texas Experimental Tokamak (TEXT) have shown that the global energy-confinement time (τ_E) saturates with increasing plasma density.[1] This trend, which has been observed in numerous other Ohmically heated tokamaks, has been attributed to the increased dominance of the ion thermal loss channel over the electron channel at sufficiently high densities. If the ion losses are taken to be governed by neoclassical transport, then transport-modeling calculations can provide predictions for the density at which τ_E saturates.[2] However, in many discharges refueled by gas puffing (e.g., DOUBLET-III[3] and ALCATOR-C[4]), the saturation of τ_E is actually observed to occur at densities considerably lower than the ion neoclassical estimates. As first proposed by Coppi *et al.*,[5] this "anomalous" behavior could be caused by the onset of enhanced ion thermal transport due to the excitation of drift instabilities driven by ion temperature gradient (η_i).[6] With the use of models based on the presence of these modes, recent transport-code calculations have yielded results in reasonable agreement with the density saturation observed in a large number of tokamak experiments.[7-9] In addition to these high-density Ohmic cases, evidence for anomalous ion thermal transport has also been found in tokamaks heated by neutral-beam injection (NBI). Specifically, charge-exchange ion-temperature–profile measurements on NBI-heated DOUBLET-III discharges have led to results that the ion thermal diffusivity is not only much larger but also exhibits a radial dependence dramatically different from that predicted by ion neoclassical theory.[10]

In light of the preceding discussion, it is clear that there is ample motivation to search for direct experimental evidence either in support of or against the proposition that η_i-type instabilities could be responsible for the anomalous ion confinement that causes the saturation of τ_E in high-density Ohmic plasmas. An obvious feature to explore is the nature of the microturbulence spectra characterizing the presence of such modes. If the parameter η_i [$=L_{n_i}/L_{T_i}=d\ln T_i/d\ln n_i$] exceeds a threshold value, $(\eta_i)_c \simeq 1$ to 2, then drift-type microinstabilities propagating in the *ion* diamagnetic drift direction are predicted to be present with a typical range of $k_\perp \rho_i \leq 1$. This is essentially the same $|k|$-space range characteristic of the usual electron-drift-wave turbulence, with $\mathbf{k}_\perp$ the wave vector of the density fluctuation in the plane perpendicular to the toroidal magnetic field and ρ_i the ion gyroradius. The primary focus of the present study is to examine systematically the density-fluctuation spectra at various plasma densities in the Ohmically heated TEXT tokamak. A unique multichannel, heterodyne, far-infrared laser scattering system is employed which allows measurement of the entire $S(k_\perp,\omega) \propto [\tilde{n}(k_\perp,\omega)]^2$ spectra during a single discharge. The main result is that an ion mode (i.e., microturbulence propagating in the ion diamagnetic drift direction) has indeed been experimentally observed along with the familiar density fluctuations propagating in the electron diamagnetic drift direction.[11,12] In the following, measured results for the magnitude of the ion mode together with its frequency and wave-vector spectra are presented and compared with the measured properties of the turbulence propagating in the electron diamagnetic drift direction. Discussions of the conditions under which the ion mode becomes prominent and of the statistical dispersion and phase velocity of the ion features are also presented.

The scattering system, which is described in detail by Brower *et al.*,[13] simultaneously collects the frequency-

shifted scattered radiation at six discrete angles corresponding to $0 \leq k_\perp \leq 15$ cm^{-1}. A twin-frequency laser source and heterodyne receiver system permit resolution of the wave-propagation direction. The portion of the far-infrared laser beam ($P_0 \simeq 20$ mW, $\lambda_0 = 2\pi/k_0 = 1222$ μm, $\Delta\omega/2\pi \simeq 1$ MHz for the heterodyne receiver) utilized as the probe beam is weakly focused along a vertical chord to a waist of radius $a_0 = 2$ cm at the e^{-2} point of the intensity distribution. The measured wave-number resolution is independent of wave vector with $\Delta k = \pm 1$ cm^{-1} ($\simeq 2/a_0$). The length of the scattering volume (along $\mathbf{k}_0$) varies as a function of wave number and ranges from ± 11 cm (e^{-1} point of scattered power) at $k_\perp = 12$ cm^{-1} to a chord average as $k_\perp \rightarrow 0$. The spatial resolution perpendicular to $\mathbf{k}_0$ is the beam radius. Scattering occurs in a plane perpendicular to the toroidal magnetic field, and for this investigation the source beam is incident upon the plasma along a vertical chord at the tokamak major radius where scattering is primarily from fluctuations with a poloidal wave vector k_θ. The TEXT tokamak has a major radius $R = 1$ m and a limiter radius $a = 27$ cm. Data presented here were taken during the plateau region of sawtoothing discharges for plasma conditions with $I_p = 400$ kA, $B_T = 28$ kG ($r_{q=1} \simeq 10$ cm, where q is the safety factor), and $2\times10^{13} \leq \bar{n}_e \leq 8\times10^{13}$ cm^{-3}, where I_p is the plasma current, B_T is the toroidal field, and $\bar{n}_e$ is the central chord-averaged electron density. The working gas is hydrogen, and the plasma current and toroidal magnetic field are parallel.

Typical microturbulence frequency spectra for poloidal fluctuations under low-density conditions ($\bar{n}_e = 2\times10^{13}$ cm^{-3}, $T_{e0} = 1.3$ keV, and T_{i0} measured to be roughly 900 eV) are shown in Fig. 1(a) at four different wave vectors corresponding to $k_\theta = 4.5$, 7, 9, and 12 cm^{-1}. The scattering volume at each wave vector is centered 25 cm above the midplane along a vertical chord at $R = 1$ m. The heterodyne receiver system permits resolution of the wave-propagation direction, with negative (positive) frequency corresponding to fluctuations propagating in the electron (ion) diamagnetic drift direction as measured in the laboratory frame of reference. At each wave vector examined, there is a distinct large-amplitude broad-band ($\Delta\omega/\omega \geq 1$) peak in the electron direction as compared with the low-level contribution from the ion direction which appears to peak at approximately zero frequency. The peak in the power spectra moves to higher (more negative) frequencies as k_θ increases indicating a dispersion for the fluctuations. It should be noted that plasma rotation effects induced by a negative plasma potential serve to shift the spectra to more negative frequencies. At this plasma density the global energy-confinement time τ_E has not saturated.[1]

In sharp contrast, a factor-of-4 increase in the plasma density to $\bar{n}_e = 8\times10^{13}$ cm^{-3} results in density fluctuation spectra of a remarkably different nature as shown in Fig. 1(b). Here the plasma current and toroidal field are unchanged from that for Fig. 1(a), although the plasma temperature has decreased to $T_{e0} \simeq 700$ eV with T_{i0} roughly around 600 eV. In addition to the large-amplitude broad-band peak observed for negative frequencies, a new separate peak now appears at positive frequencies to the ion diamagnetic drift direction. The magnitude of the ion feature is of the same order as the electron feature. It is broad band ($\Delta\omega/\omega \simeq 1$), and the power spectra move to higher (more positive) frequencies as k_θ increases. Removal of plasma-rotation effects would make the ion feature appear at larger positive frequencies. Under these conditions, τ_E exhibits high-density saturation.[1]

In order to describe further the new ion feature, it is now worthwhile to examine the statistical dispersion of the fluctuations as shown in Fig. 1(c). This is obtained by our plotting the mean frequency $[\bar{\omega}_k = \sum\omega S_k(\omega)/\sum S_k(\omega)]$ against the wave vector for both the ion and

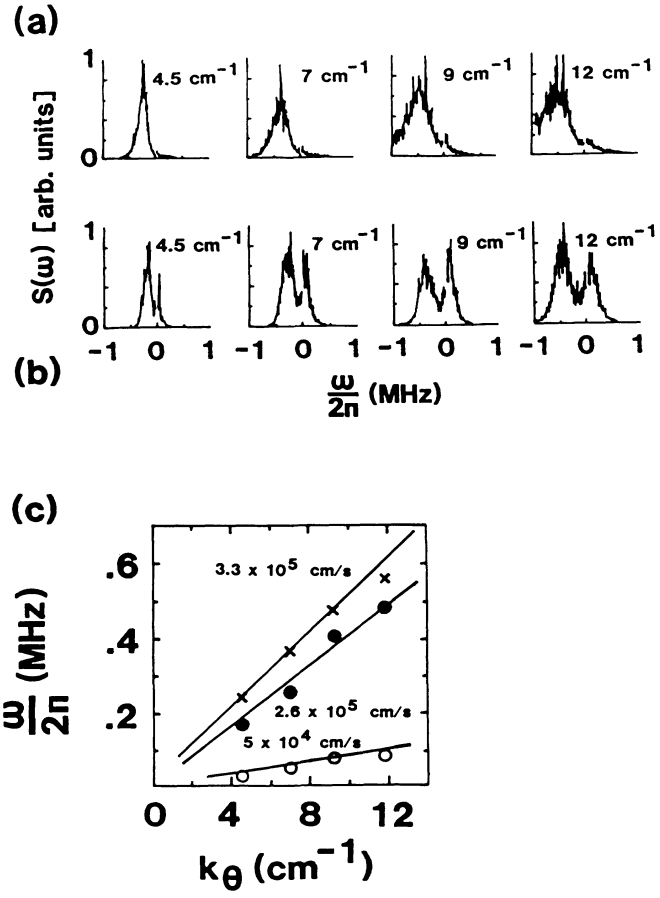

FIG. 1. Frequency spectra for discharge conditions $I_p = 400$ kA, $B_T = 28$ kG and (a) $\bar{n}_e = 2\times10^{13}$ cm^{-3}, (b) $\bar{n}_e = 8\times10^{13}$ cm^{-3}. Negative frequency corresponds to the electron diamagnetic drift direction. (c) Microturbulence statistical dispersion for electron component (2×10^{13} cm^{-3}, crosses), electron component (8×10^{13} cm^{-3}, filled circles), and ion component (8×10^{13} cm^{-3}, open circles).

electron features. For the low-density discharge, the measured phase velocity of the electron feature is $v_e \simeq 3.3\times10^5$ cm/s, while the low-amplitude ion feature demonstrated no clear dispersion. At the high-density condition, the electron feature has a measured $v_e \simeq 2.6\times10^5$ cm/s as compared to the ion feature with $v_i \simeq 5\times10^4$ cm/s. Both the electron and ion components exhibit an essentially linear dispersion The maximum electron diamagnetic drift velocity computed with use of TEXT profiles for the high- (low-) density discharge is v_{De} $(=\omega_e^*/k_\theta = T_e/eBL_n) \simeq 5\times10^4$ (1.2×10^5) cm/s.

By the integration of $S_k(\omega)$ over negative and positive frequencies separately and by looking at their ratio, it is possible to quantify the relative strengths of the two components. As illustrated in Fig. 2(a), the ratio of electron to ion contributions (S_e/S_i) is plotted against the wave vector at three different values of density. At plasma density $\bar{n}_e = 2\times10^{13}$ cm^{-3}, the ratio is $S_e/S_i \simeq 13$. This is dramatically reduced to $S_e/S_i \simeq 2$ for $\bar{n}_e \simeq 8\times10^{13}$ cm^{-3}. For an intermediate density of $\bar{n}_e = 5\times10^{13}$ cm^{-3}, the ratio is $S_e/S_i \simeq 8$. As the electron density is increased, the ion contribution grows. However, it does not become prominent (i.e., a distinct peak is not observed in the ion-drift direction) until $\bar{n}_e > 5\times10^{13}$ cm^{-3}. The density dependence of the electron and ion contributions is shown in Fig. 2(b) for $k_\theta = 12$ cm^{-1}. Similar observations are made at the other measured values of k_θ. In terms of the frequency-integrated wave-vector spectra, however, Fig. 2(c) shows that the normalized $S(k_\theta)$ are essentially unchanged from low to high density. At high densities, both the electron $[S_e(k_\theta)]$ and ion $[S_i(k_\theta)]$ contributions individually possess the same functional dependences as $S(k_\theta)$ $[=S_e(k_\theta)+S_i(k_\theta)]$. The mean wave vector in both instances is $\bar{k}_\theta \simeq 3$ cm^{-1}, which for fluctuations peaking outside $r_{q=1}$ implies $0.1 \le \bar{k}_\theta \rho_s \le 0.4$ where $\rho_s = (M_i T_e)^{0.5}/eB$. The falloff at large poloidal wave numbers goes roughly as $k_\theta^{-(3\pm1)}$.

The electron-density and -temperature profiles are shown in Figs. 3(a) and 3(b). It is important to note that the density profile appreciably broadens as n_e is increased, while the electron temperature profile is essentially constant. This is seen more clearly in Figs. 3(c) and 3(d), where the scale lengths are plotted versus radial position. The broader n_e profile at high density results in longer scale lengths over a large portion of the cross section, whereas L_{T_e} remains roughly unchanged. Hence, η_e is clearly larger in the high-density case. Unfortunately, similar estimates for η_I cannot be made as T_i profiles are currently unavailable. Nevertheless, there is at least some indirect evidence that η_i could be near the theoretical stability threshold $(\eta_i)_c$ at low density and well above $(\eta_i)_c$ at high density. For the low-density discharge, η_e values are typically less than 3 outside $r_{q=1}$. Since $T_i < T_e$ at the plasma center and $T_i \simeq T_e$ at the plasma edge, it can be inferred that $\eta_i < \eta_e$ in these cases. For this reason, η_i is likely to be close to $(\eta_i)_c$, which itself has only been roughly estimated theoretically to be about 2. If only weakly unstable, the associated η_i-mode-driven turbulence could easily be masked by the usual electron-drift-wave-type fluctuations which can coexist. Consequently, the experimental observations of a very small ion feature under these conditions tend to correlate with the theoretical expectation. For the high-density discharge, $\eta_e \ge 3$ for $r_{q=1} < r < 20$ cm. Since T_i is likely to be more strongly coupled to T_e from collisionality considerations, η_i is probably closer to η_e than for the low-density discharge. As such, in certain regions of the plasma, η_i could well be sufficiently above threshold to give rise to significant turbulent transport. Hence, the experimental measurement of a strong ion feature here lends support to the theoretical proposition that the observed saturation of τ_E could be due to enhanced thermal losses in the ion channel generated by η_i-type instabilities.

The preceding arguments are by no means rigorously

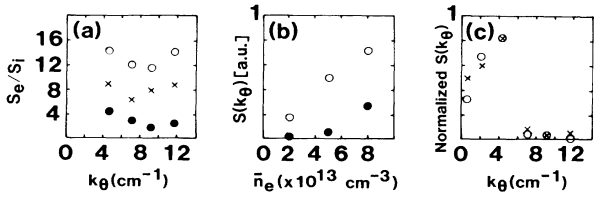

FIG. 2. (a) Ratio of electron to ion components at $\bar{n}_e = 2\times10^{13}$ cm^{-3} (open circles), 5×10^{13} cm^{-3} (crosses), and 8×10^{13} cm^{-3} (filled circles). (b) Density dependence of the electron (S_e, open circles) and ion (S_i, filled circles) components for $k_\theta = 12$ cm^{-1}. (c) Normalized $S(k_\theta)$ $[=S_e(k_\theta)+S_i(k_\theta)]$ at $\bar{n}_e = 2\times10^{13}$ cm^{-3} (crosses) and 8×10^{13} cm^{-3} (open circles).

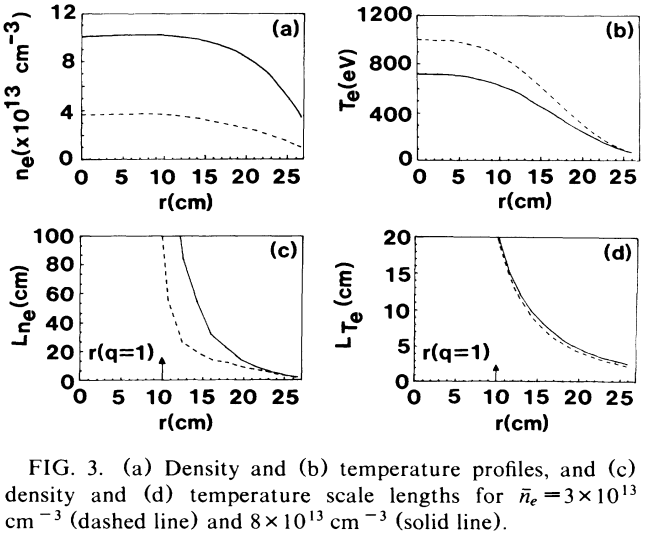

FIG. 3. (a) Density and (b) temperature profiles, and (c) density and (d) temperature scale lengths for $\bar{n}_e = 3\times10^{13}$ cm^{-3} (dashed line) and 8×10^{13} cm^{-3} (solid line).

conclusive in establishing the connection between the measured ion feature and the theory of η_i-mode–driven turbulence. Nevertheless, it is quite encouraging that there are no obvious aspects of the experimental results which appear directly to contradict this relationship. For example, measurements of the wave-vector spectra indicating $0.1 \leq \bar{k}_\theta \rho_s \leq 0.4$ and a falloff proportional to $k_\theta^{-(3\pm1)}$ are in reasonable agreement with recent analytical computations yielding $(k_\theta \rho_s)_{\rm rms} \simeq 0.4$ and a falloff proportional to $k_\theta^{-2.5}$.[14] In addition, fluctuation measurements on ALCATOR-C have shown a change in group velocity from the electron to ion diamagnetic drift direction at high densities.[15] Further experimental evidence from TEXT relevant to this issue will come from (i) planned measurements of the ion-temperature profile, which could provide direct information about η_i and the ion thermal diffusivity, χ_i, and (ii) pellet-injection refueling experiments, which could possible control the strength of the ion feature by significant modifications of the density profile. Note that if these future data were to contradict the η_i-mode theory, it would open up the question of what physics is responsible for the new ion feature presented in this Letter.

The extended interaction volume lengths and limited spatial scans available with a heterodyne receiver have prevented accurate measurements of the spatial localization of the ion mode. Nevertheless, it appears to exist over a large portion of the plasma radius. Langmuir-probe measurements in the extreme edge and scrapeoff regions of TEXT observe a shear layer outside of which the fluctuations are observed to be propagating in the ion-drift direction.[16] This is due to an $\mathbf{E}\times\mathbf{B}$ Doppler shift which changes sign across the shear boundary. Although the extended interaction length of the scattering volume encompasses this narrow layer ($\simeq 2$ cm), it is not thought that these fluctuations contribute significantly to the scattering observations of the ion feature for several reasons.[15] First, the phase velocity measured for the ion feature by scattering does not agree with that observed by the probes for fluctuations in the limiter shadow. Second, measurement of the $\tilde{n}$ distribution in the limiter shadow at low and high densities does not exhibit the qualitative change necessary to make the ion feature prominent at high density while being negligible at low density. Finally, since the scrapeoff plasma involves a very narrow region compared to the entire scattering volume length and since the density is low there, it is unlikely that fluctuations from this region could dominate the measured spectra.

In summary, a distinct ion mode has been identified in the fluctuation spectra measured on the Ohmically heated TEXT tokamak. The onset of this ion feature correlates with the observed saturation of τ_E at high density. Comparison of its measured spectral characteristics with theoretically predicted properties of η_i-mode–driven turbulence yields reasonable agreement. Further evidence either for or against the proposition that the η_i-type instabilities are responsible for the enhanced ion thermal transport causing the saturation of τ_E is expected to come from experiments scheduled in the near future on TEXT.

The authors have greatly appreciated the assistance of R. L. Savage, Jr., in the development and installation of the twin-frequency laser necessary for heterodyne detection. Machine operation time and technical support were generously provided by the Fusion Research Center, University of Texas, Austin, under the direction of A. J. Wootton. This work was supported by the U.S. Department of Energy, Office of Fusion Energy under Contract No. DE-AC05-78ET53043, through Subcontract No. UT-1-24120-52019.

[1]R. V. Bravenec *et al.*, Plasma Phys. Controlled Fusion **27**, 1335 (1985).

[2]R. E. Waltz and G. E. Guest, Phys. Rev. Lett. **42**, 651 (1979).

[3]S. Ejima *et al.*, Nucl. Fusion **22**, 1627 (1982).

[4]S. M. Wolfe *et al.*, Nucl. Fusion **26**, 329 (1986).

[5]B. Coppi *et al.*, in *Proceedings of the Tenth International Conference on Plasma Physics and Controlled Nuclear Fusion Research, London, 1984* (International Atomic Energy Agency, Vienna, 1985), Vol. 2, p. 93.

[6]L. I. Rudakov and R. Z. Sagdeev, Dokl. Akad. Nauk SSSR **138**, 581 (1961) [Sov. Phys. Dokl. **6**, 415 (1961)]; B. Coppi, M. N. Rosenbluth, and R. Z. Sagdeev, Phys. Fluids **10**, 582 (1967).

[7]F. Romanelli, W. M. Tang, and R. B. White, Nucl. Fusion **26**, 1515 (1986).

[8]R. R. Dominguez and R. E. Waltz, Nucl. Fusion **27**, 65 (1987).

[9]M. H. Redi *et al.*, Princeton Plasma Physics Laboratory Report No. PPPL-2368, 1987 (unpublished).

[10]R. J. Groebner *et al.*, Nucl. Fusion **26**, 543 (1986).

[11]D. L. Brower *et al.*, Phys. Rev. Lett. **54**, 689 (1985).

[12]D. L. Brower, W. A. Peebles, and N. C. Luhmann, Jr., University of California at Los Angeles Institute of Plasma and Fusion Research Report No. PPG-1050, 1987 (to be published).

[13]D. L. Brower *et al.*, in "Infrared and Millimeter Waves," edited by K. J. Button (Academic, New York, to be published).

[14]G. S. Lee and P. H. Diamond, Phys. Fluids **29**, 3291 (1986).

[15]R. L. Watterson *et al.*, Phys. Fluids **28**, 2857 (1985).

[16]C. P. Ritz *et al.*, to be published.